Journal of Thermal Analysis and Calorimetry, Vol. 58 (1999) 249-256

STUDY ON THE MELTING PROCESS OF NITROCELLULOSE BY THERMAL ANALYSIS METHOD

N. Binke[1,2*], *L. Rong*[3], *C. Xianqi*[2], *W. Yuan*[2], *Hu Rongzu*[2] *and Y. Qingsen*[1]

[1]Department of Chemistry, Zhejiang University, Hangzhou 310027
[2]Xian Modern Chemistry Research Institute, Xian 710065
[3]Department of Food Engineering, Nanchang University, Nanchang 330047, P. R. China

Abstract

The melting process of NC is studied by using modulated differential scanning calorimetry (MDSC) technique, the microscope carrier method for measuring the melting point and the simultaneous device of the solid reaction cell in situ/RSFT-IR. The results show that the endothermic process in the MDSC curve is reversible. It is caused by the phase change from solid to liquid of the mixture of initial NC, decomposition partly into condensed phase products. The values of the melting point, melting enthalpy (ΔH_m), melting entropy (ΔS_m), the enthalpy of decomposition (ΔH_{dec}) and the heat-temperature quotient (ΔS_{dec}) obtained by the MDSC curve of NC at a heating rate of 10 K min^{-1} are 476.84 K, 205.6 J g^{-1}, 0.4312 J g^{-1} K^{-1}, –2475.0 J g^{-1} and –5.242 J g^{-1} K^{-1}, respectively. The MDSC results of NC with different nitrogen contents show that with increasing the nitrogen content in NC, the absolute values of ΔH_m, ΔS_m, ΔH_{dec} and ΔS_{dec} increase.

Keywords: MDSC, melting process, microscope carrier method, NC, simultaneous device of solid reaction cell/RSFT-IR

Introduction

With regard to the problem whether the melting point of nitrocellulose (NC) exists or not, there are two points of view: (1) Huilu [1], Baoguan [2] and Morrow *et al.* [3, 4] considered that the melting point of NC cannot be determined because NC does not melt; (2) Binhe *et al.* [5] measured the melting point of NC by the polarizing microscope, infrared spectroscopy (IR) and differential thermal analysis-thermogravimetry (DTA-TG) techniques, and pointed out that the melting point of NC exists and first melting takes place and then decomposes. In order to test and verify the above-mentioned views, we investigated the melting process of NC by modulated differential scanning calorimetry (MDSC) technique, the microscope carrier

---

[*] Authors to whom all correspondence should be addressed N. Binke and H. Rongzu.

1418–2874/99/ $ 5.00

Akadémiai Kiadó, Budapest
Kluwer Academic Publishers, Dordrecht

method for measuring the melting point and the simultaneous device of the solid reaction cell in situ/rapid-scan Fourier transform infrared spectroscopy (RSFT-IR).

Experimental

Materials

The highly nitrated NC containing 14.14 and 13.78% of nitrogen used in this work were prepared and purified at our institute in Xian and other NC containing 13.54, 12.97 and 11.92% of nitrogen were provided by Huian Chemical Factory in Xian, China.

Instruments

The determination of the melting process of NC was carried out on a Mettler's Model PF5 microscope carrier for measuring the melting point, MDSC instrument (Model TA2100, TA Co. USA) and the solid reaction cell in situ (Xiamen University, Xiamen, China) in conjunction with RSFT-IR (Model 60SXR FT-IR, Nicolet Co.). The operation for the microscope carrier method was: heating rate, 2 K min^{-1}; multiplication constant, 100. For MDSC: the sample mass, about 1 mg; heating rate, 10 K min^{-1}; reference sample, α-Al$_2$O$_3$; atmosphere, a flowing rate of

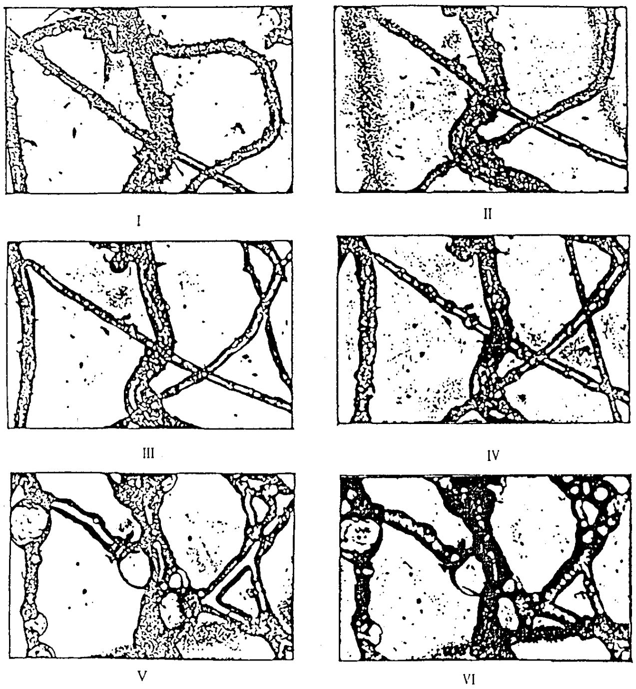

Fig. 1 Photographs of NC (14.4% N) obtained by the microscope carrier method at room temperature (I), 465 (II), 469 (III), 470 (IV), 472 (V) and 476 K(VI)

50 ml min^{-1} of N_2 ; modulation, sine; amplitude, ±1.061 K; period, 40 s. The operation for the solid reaction cell in situ/RSFT-IR was: the sample mass, about 0.7 mg; sample/KBr (mass ratio), 1:100; heating rate, 20 K min^{-1}. The experiments were conducted in the solid reaction cell in situ without cover, 18 files min^{-1} and 8 scans $file^{-1}$ were recorded at a resolution of 4 cm^{-1}, and infrared spectra of NC were obtained using DTGS detector.

Results and discussion

The photographs of NC (14.14% N) obtained by the microscope carrier method at different temperatures are presented in Fig. 1. It is clear that during the uniform heating of NC, the fibers of NC at room temperature (Fig. 1–I) were longer and were gradually straightened, and expanded with some small liquid drops appearing. Then the fibers became transparent (Figs 1–II, III) and emitted bubbles, being gas phase decomposition products. The system was changed completely into liquid (Figs 1–IV, V). Finally the fibers stopped bubbling, straightened and became transparent completely, and the remnants were turned into glue with their colour deepened (Fig. 1–VI). These phenomena reveal that NC melted and was accompanied by the complicated decomposition process during heating.

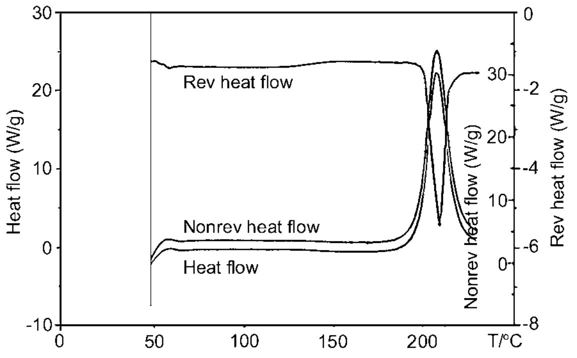

Fig. 2 Typical MDSC curves of NC (14.14% N) at a heating rate of 10 K min^{-1}

The typical MDSC curves of NC (14.14, 13.54, 12.97 and 11.92% N) at a heating rate of 10 K min^{-1} are presented in Figs 2–5. In the MDSC curves, the inverse endothermic process was attributed to the melting of NC, and the irreversible exothermic process was attributed to the decomposition of NC. The thermodynamic data determined by MDSC, including the melting point (T_m), melting enthalpy (ΔH_m), melting entropy (ΔS_m), extrapolated to onset temperature (T_e), enthalpy of decomposition (ΔH_{dec}) and the heat-temperature quotient (ΔS_{dec}), are all listed in Table 1.

The data in Table 1 suggest that with increasing the nitrogen content in NC, the absolute values of ΔH_m, ΔS_m, ΔH_{dec} and ΔS_{dec} increase. The fact that T_m is higher than T_c shows that NC has decomposed partly before melting, and the melting process is that of the mixture of the original NC and its decomposition products in coacervate phase. The values of T_m in Table 1 are actually melting points of the mixtures.

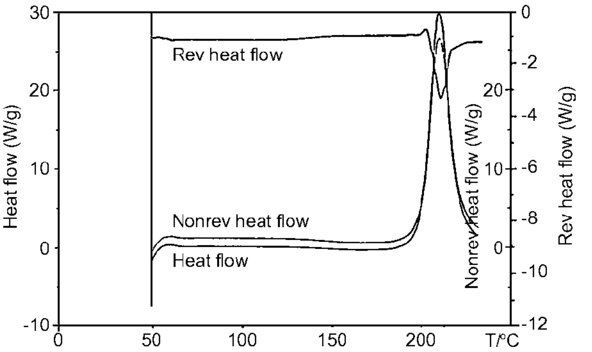

Fig. 3 Typical MDSC curves of NC (13.54% N) at a heating rate of 10 K $\min^{-1}$

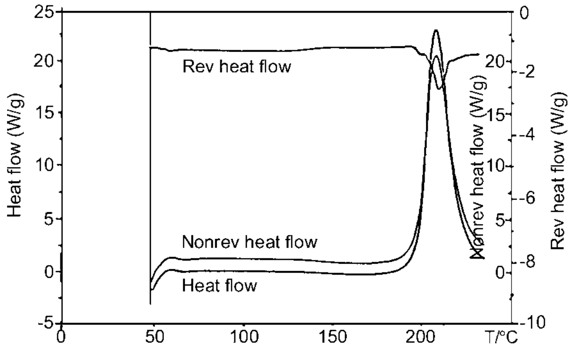

Fig. 4 Typical MDSC curves of NC (12.97% N) at a heating rate of 10 K $\min^{-1}$

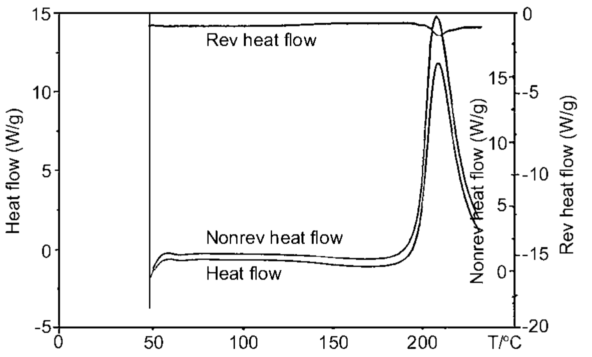

Fig. 5 Typical MDSC curves of NC (11.92% N) at a heating rate of 10 K $\min^{-1}$

Table 1 Thermodynamic data of NC determined by MDSC

Sample NC/%N	Melting process			Decomposition process		
	T_m/K	ΔH_m/ J g^{-1}	ΔS_m/ J g^{-1} K^{-1}	T_e/K	$-\Delta H_{dec}$/ J g^{-1}	$-\Delta S_{dec}$/ J g^{-1} K^{-1}
14.14	476.84	205.6	0.4312	472.18	2475.0	5.242
13.54	478.59	119.0	0.2486	472.07	2402.6	5.089
12.97	479.69	74.9	0.1561	471.46	2053.9	4.356
11.92	478.91	40.3	0.0841	470.15	1598.3	3.400

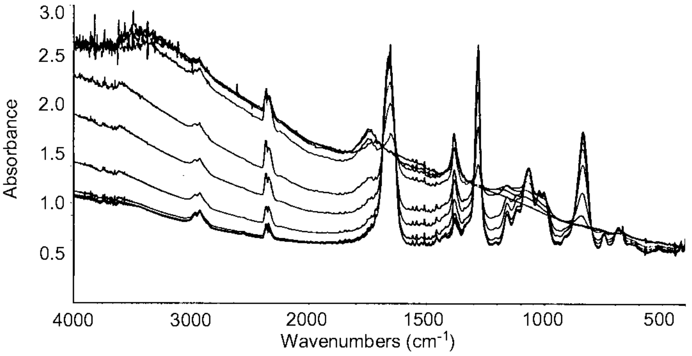

Fig. 6 IR spectra of the decomposition products in coacervate phase during the thermal decomposition process of NC (14.14% N) at a heating rate of 20 K min^{-1} (collecting times of IR spectra from bottom to top is 5.36, 5.93, 6.50, 6.78, 7.06, 7.35, 7.63, 7.94, 8.19, 8.48, 8.76, 9.33, 12.67 min, respectively)

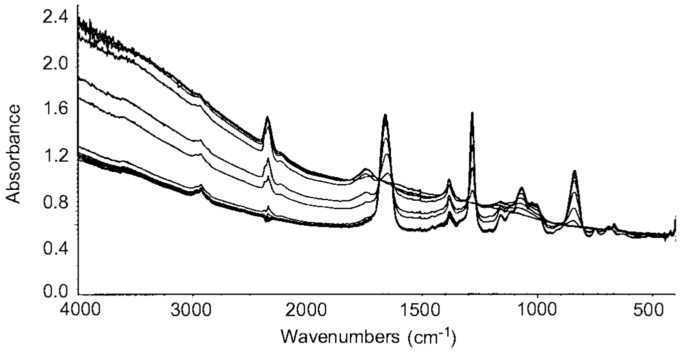

Fig. 7 IR spectra of the decomposition products in coacervate phase during the thermal decomposition process of NC (13.54% N) at a heating rate of 20 K min^{-1} (collecting times of IR spectra are the same as Fig. 6)

Besides the above-mentioned method, the melting process of NC was also investigated by the solid reaction cell in situ without cover. The obtained spectra (Figs 6–9)

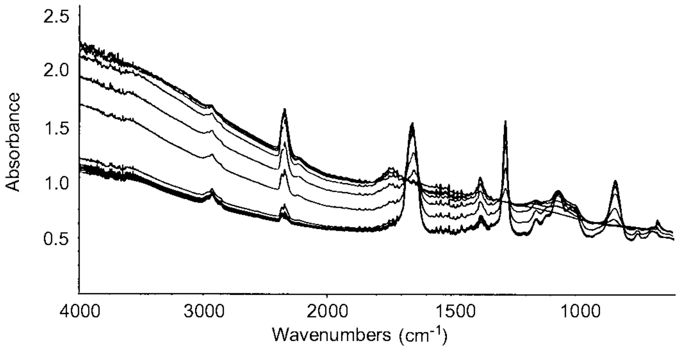

Fig. 8 IR spectra of the decomposition products in coacervate phase during the thermal decomposition process of NC (12.97% N) at a heating rate of 20 K min^{-1} (collecting times of IR spectra are the same as Fig. 6)

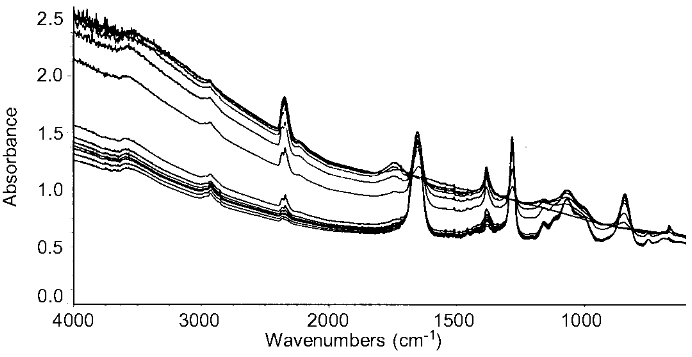

Fig. 9 IR spectra of the decomposition products in coacervate phase during the thermal decomposition process of NC (11.92% N) at a heating rate of 20 K min^{-1} (collecting times of IR spectra are the same as Fig. 6)

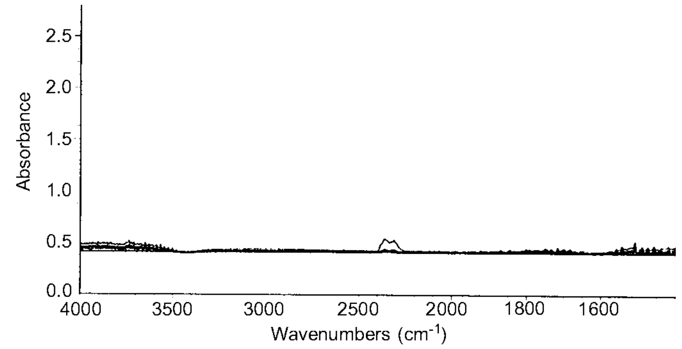

Fig. 10 IR spectra in the thermal decomposition process of KBr at a heating rate of 20 K min^{-1} (collecting times of IR spectra from bottom to top is 0.04, 0.66, 3.61, 6.72, 8.84, 12.95 min, respectively)

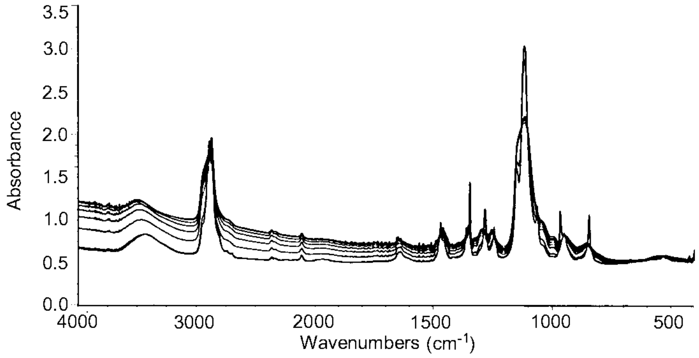

Fig. 11 IR spectra in the thermal decomposition process of PEG 1500 at a heating rate of 20 K min^{-1} (collecting times of IR spectra from bottom to top is 0.05, 0.61, 1.18, 1.75, 2.32, 2.89, 3.45, 5.16 min, respectively)

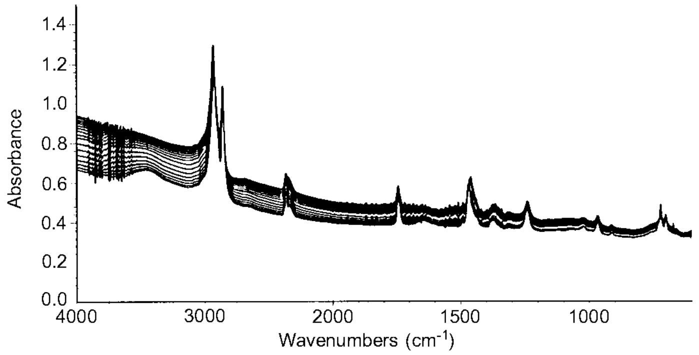

Fig. 12 IR spectra in the thermal decomposition process of EVA at a heating rate of 20 K min^{-1} (collecting times of IR spectra from bottom to top is 0.12, 0.55, 0.96, 1.38, 1.80, 2.22, 2.63, 3.05, 3.47, 3.89, 4.30, 4.72, 5.14, 5.56, 5.97, 6.38, 6,81, 7.18 min, respectively)

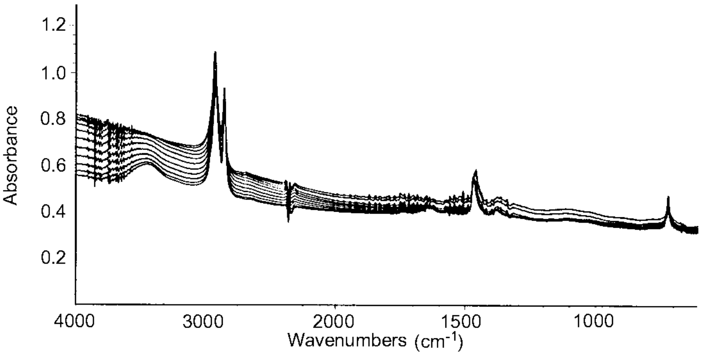

Fig. 13 IR spectra in the thermal decomposition process of PE at a heating rate of 20 K min^{-1} (collecting times of IR spectra from bottom to top is 0.12, 0.55, 0.96, 1.38, 1.80, 2.22, 2.63, 3.05, 3.47, 5.14, 6.81 min, respectively)

of the thermal decomposition products in coacervate phase show the baselines of IR make a sudden leap toward the decrease of transmissivity in the temperature range from 426 to 447 K. In order to confirm the sudden leap owing to the melting of NC, we collected the spectra of the tablet of KBr, and the mixtures of KBr variously with polyethylene glycol (PEG 1500), polyethylene (PE), ethylene vinyl acetate copolymer (EVA) (Figs 10–13) under the same conditions as that of NC. The results show that similar sudden leaps of baselines in IR spectra of these polymers take place in their individual temperature ranges of melting process, the process is a liquefaction process and the temperature range of the sudden leap is the temperature range of melting process. In the beginning of the sudden leap of baseline, the intensity value of $O–NO_2$ group has decreased, which suggests that NC had decomposed partly before melting.

Conclusions

On the basis of the results obtained by microscope carrier method, MDSC and the solid reaction cell in situ/RSFT-IR, it is confirmed that NC decomposes partly before melting, and the melting is accompanied by decomposition. The so-called ‘melting point’ of NC is melting point of the mixture of the original NC and its decomposition products.

References

1 Wu Huilu, ‘Nitrocellulose’, The Press of National Defense, Beijing 1974, p. 47.
2 Li Baoguan and Fu Ruonong, ‘The Chemistry and Technology of Nitroglycerine and Nitrocellulose’, The Editorial Department of Beijing Science and Technology, Beijing 1962, p. 99.
3 S. I. Morrow, Microscope, 21 (1973) 229.
4 S. I. Morrow, Microscope, 22 (1974) 349.
5 Luo Binhe, Liu Jihua et al., J. Beijing Institute of Technology, 16 (1996) 259.